IEEE Access
Multidisciplinary ⋮ Rapid Review ⋮ Open Access Journal

Received 17 September 2023, accepted 5 October 2023, date of publication 10 October 2023, date of current version 18 October 2023.

Digital Object Identifier 10.1109/ACCESS.2023.3323430

RESEARCH ARTICLE

Millimeter Wave Planar Wideband Circularly Polarized Antenna Loaded Triangular Patch for End-Fire Radiation

HENGFEI XU[1], (Member, IEEE), BOYU SIMA[2], (Member, IEEE), PU WEI[1], LEI TANG[1], SHU JIANG[1], AND CHUANQING LIU[1]

[1]College of Information and Communication Engineering, Nanjing Institute of Technology, Nanjing 211167, China
[2]School of Electronic and Optical Engineering, Nanjing University of Science and Technology, Nanjing, Jiangsu 210094, China

Corresponding author: Hengfei Xu (xhf201@163.com)

This work was supported in part by the Natural Science Foundation of Jiangsu Province under Grant BK20191011, in part by the Scientific Research Foundation of Nanjing Institute of Technology under Grant YKJ201869, and in part by the Natural Science Foundation of the Jiangsu Higher Education Institutions of China under Grant 22KJB510023.

ABSTRACT A planar wideband circularly polarized (CP) end-fire antenna is presented for millimeter-wave (mm-wave) applications. First, the antenna consists of an open-ended substrate integrated waveguide (SIW) feeding line in the middle, a pair of stacked substrates with shorted triangular patches on both upper and lower sides, and an offset parallel strip. The shorted triangular patch is viewed as a horizontally polarized electric dipole, while the open-ended SIW is equivalent to an enhanced magnetic dipole due to the stacked substrates. Wide axial ratio (AR) performance is achieved by simultaneously exciting the two dipoles with orthogonal phase supplied by the offset parallel strip. Then, working principle and parameter analysis are explained and discussed for a further understanding. Finally, a prototype is fabricated and measured to verify the design scheme, which demonstrates wide AR bandwidth performance of 38.6%, novel and efficient radiating structure, simple and compact antenna size, and easy fabrication and integration. This indicates that the proposed antenna is a promising candidate to design wideband end-fire CP antenna in the mm-wave frequency band.

INDEX TERMS Circularly polarized, end-fire antenna, millimeter wave, triangular patch.

I. INTRODUCTION

With the rapid development of communication technology, especially the fifth-generation mobile communication system (5G) and 5G-beyond (B5G), millimeter wave (mm-wave) has become one of the hottest antenna design bands [1], [2]. Owing to the ample spectrum resources, reduced multi-path interference, lower polarization mismatch, and the ability in duplex applications, mm-wave circularly polarized (CP) antennas demonstrate superior performance in stable wireless links when compared to linearly polarized (LP) antennas [3]. A signal misalignment in polarization mismatch and degradation between the receiver and transmitter could exist, when LP antennas are employed [4]. The concept of realizing a CP antenna is simultaneously excited by two cross-arranged LP modes with an orthogonal phase in the radiating direction. Based on the idea, many CP antenna elements, such as patches [5], slots [6], spirals [7], magnetic-electric (ME) dipoles [8], dielectric resonator antennas [9], are developed. Another method using sequential feedings can provide orthogonal phase delay, making it simple to realize CP array [10]. The orthogonal modes are arranged in a two-dimensional plane perpendicular to the direction of propagation. However, since many wireless devices require a radiation beam parallel to the antenna, it is necessary to research CP antenna with end-fire radiation.

Inspired by CP antennas with broadside radiation, some simple combinations can also produce end-fire CP wave, such as the combination of two orthogonal magnetic dipoles [11], the combination of a magnetic dipole and a V-shape open

The associate editor coordinating the review of this manuscript and approving it for publication was Shah Nawaz Burokur.

loop [12], and offset parallel strips with proper dielectric loading [13]. The end-fire CP antennas have a single CP resonant point, resulting in a limited bandwidth. Dielectric rod antennas effectively resolve the issue of CP bandwidth limitations and exhibit desirable front-to-back ratio (FTBR) characteristics. However, the dielectric possess a complex 3D structure, and mass manufacturing is challenging [14]. Planar antenna and substrate integrated waveguide (SIW) antenna are easily manufactured and integrated with the circuit, making them a widely usage in various antenna designs, such as dual-mode planar patches [15], complementary antennas [16], [17], [18], [19], dipoles [20], [21], [22], tapered slot antennas [23], [24], [25], [26]. A dual-resonant CP antenna was developed, exhibiting an impedance bandwidth of 24.8% and a 3 dB axial ratio (AR) bandwidth of 18.8% with a lower gain of 3 dBic, as reported in [15]. Similarly, reference [16] also reported a low CP gain. To enhance the gain and FTBR of the planar antenna, a dielectric rod structure was integrated in front of antenna aperture, resulting in a significant 6 dB improvement, as described in [17]. However, the incorporation of the dielectric rod significantly enlarges dimensions in the main beam direction. Adding a tapered slot radiator on both sides of the low-profile substrate layer is an alternate approach to enhance performance [23]. This addition excites two almost equal electric field components, leading to a substantial improvement in terms of gain and FTBR performance. Importantly, a parasitic director is introduced near the printed dipole to expand the AR bandwidth of the CP element at higher frequency [25]. However, this approach involves printed circuit board (PCB) technology and metal processing technology, resulting in an increased processing cost.

Besides the AR bandwidth, gain, manufacturing process, and cost, there are other considerations, including antenna structures [27], [28], [29], [30], application scenarios [31], multibeam arrays [32], [33], reconfigurable characteristics [34], dual-CP [35], [36], [37], and bidirectional radiation [38], [39], etc. A non-planar helix antenna was investigated in [28] which radiates an end-fire CP wave and obtains an AR bandwidth of up to 46%. A CP quasi-Yagi antenna was proposed in [33] for achieving a multibeam scanning function. This antenna configuration includes one driven element and two parasitic elements, enabling a scanning angle of up to 60°. A dual-CP end-fire antenna element was designed for broadband mm-wave applications, incorporating broadband SIW Butler matrix to achieve a multibeam function [35]. The end-fire CP antenna possesses a wide range of evaluation parameters, diverse functionalities, and versatile application scenarios, thus highlighting its significant role in wireless systems.

This paper presents a novel planar wideband CP antenna with end-fire radiation pattern in mm-wave band. Two additional substrates with shorted triangular patches are pressed against both sides of the open-ended SIW substrate to form the designed antenna structure. The offset parallel strip line serves as an exciting channel that connects the electric and magnetic dipoles, while keeping them in quadrature phase. Therefore, a CP radiation beam is formed. This paper is organized as follows. Section II presents the antenna geometry, the CP working principle, and the parameter analysis. In Section III, the measured and simulated results of the proposed antenna are described, and compared with other literature works. Finally, Section IV gives a conclusion.

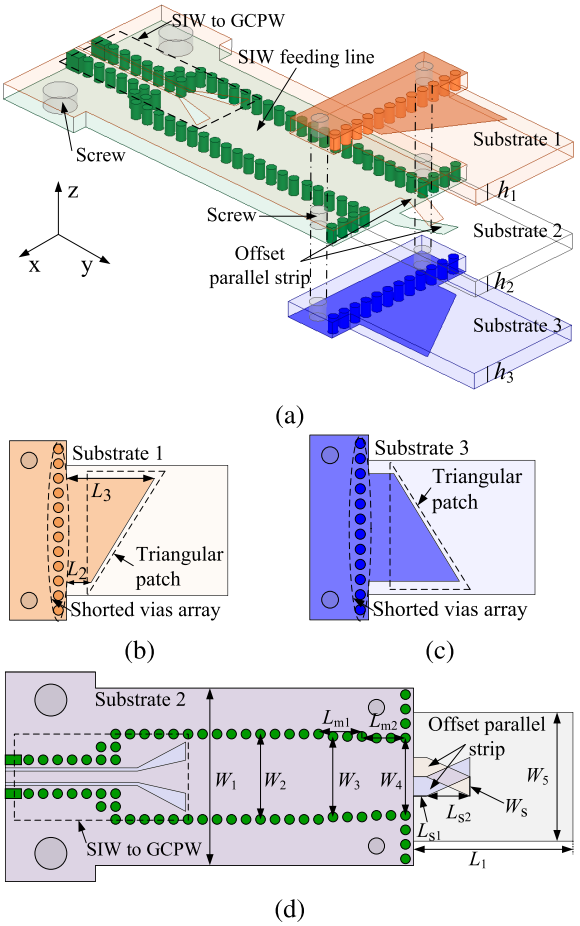

FIGURE 1. Geometry of the proposed end-fire CP antenna, (a) perspective view, (b) top view details of substrate 1 layer, (c) top view details of substrate 3 layer, (d) top view details of middle substrate 2 layer, $W_1 = 11$, $W_2 = 5.3$, $W_3 = 5.1$, $W_4 = 4.9$, $W_5 = 8$, $W_s = 1.2$, $L_1 = 9.9$, $L_2 = 1.4$, $L_3 = 5.4$, $L_{s1} = 1.2$, $L_{s2} = 2.7$, $L_{m1} = 2.7$, $L_{m2} = 2.7$, $h_1 = 1.016$, $h_2 = 1.016$, $h_3 = 1.016$. (Unit:mm).

II. ANTENNA GEOMETRY AND DESIGN

A. ANTENNA GEOMETRY

The geometry and detailed view of the wideband planar end-fire CP antenna, along with its SIW feeding network are presented in Fig. 1. A pair of shorted triangular patches are symmetrically etched on the top layer of substrate 1 and on the bottom layer of substrate 3, respectively. Each side of the triangular patch is connected to the metal surface of substrate 2 through metal vias. The feeding network of the antenna is located in the middle layer substrate 2. The end of the SIW feeding network is narrow and open, facilitating impedance matching. One end of an offset parallel strip line connects to the metal surface of the opened SIW, while the

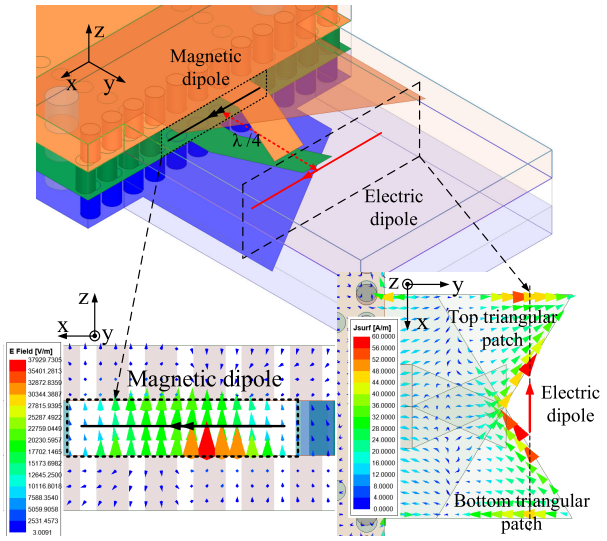

FIGURE 2. Working principle of the wideband end-fire CP antenna.

other end extends near the hypotenuse of the triangular patch, remaining in an open-circuit state. Through this structure, the energy in the SIW line is transferred to the shorted triangular patch. Because the end-fire CP antenna is implemented by stacking the three substrates together, this antenna structure can be easily processed by using single layer PCB technology.

B. CP WORKING PRINCIPLE OF THE END-FIRE ANTENNA

End-fire CP antennas often employ dipole structures due to their inherent simplicity. The antenna presented in this paper can also be regarded as a dipole structure. In the antenna design scheme, we focus on factors such as simple structure, compact size, ease of fabrication, and excellent performance. The basic design idea is as follows: Traditional SIW end-fire CP antenna consists of an electric dipole and a magnetic dipole [16]. The magnetic dipole is realized using an open-ended SIW, where the electric field is oriented perpendicular to the substrate. The curved stubs etched on both the top and bottom surfaces form the printed electric dipole, whose electric field direction is parallel to the substrate. The structure is influenced by the substrate thickness, resulting in a reduced vertical polarization electric field and narrower bandwidth. The performance of the antenna can be improved by adjusting the two orthogonal electric fields through several methods, such as increasing the length and thickness of the dielectric substrate [17], introducing a 3D printed dielectric rod [14], and adding a tapered slot radiator [25]. However, these methods lead to large antenna size, 3D antenna configuration, and increased manufacturing cost.

This paper focuses on increasing the vertical polarized electric field, denoted as a magnetic dipole, by employing stacked substrates at the antenna aperture. In addition, the horizontal electric field is achieved through a shorted triangular patch, known as an electric dipole, as displayed in Fig. 2. The working principle of the proposed antenna is

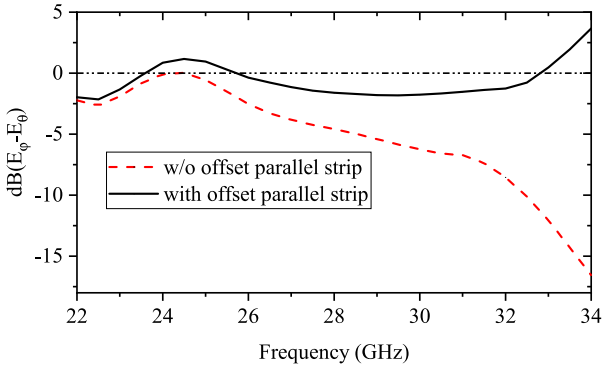

FIGURE 3. The magnitude difference of the two dipoles with and without the offset parallel strip.

illustrated by the interaction between the electric dipole and the magnetic dipole.

Compared to a single-layer structure, the stacked substrates increase radiation aperture of the magnetic dipole, leading to significantly enhanced antenna performance. However, because triangular patch is far from the SIW aperture, the horizontal electric field cannot be excited effectively. In order to solve the excitation problem, an offset strip line is designed to transfer the energy from the open-ended SIW line to the triangular patch, thereby efficiently exciting the horizontal electric field. Fig. 3 shows the magnitude difference of two dipoles with and without the offset parallel strip. E_φ and E_θ represent the far-field electric field of the electric dipole and the magnetic dipole, respectively. It can be observed that the strength of E_φ produced by the shorted triangular patch is much weaker than that of E_θ produced by the open-ended SIW, when without the offset parallel strip lines. By adjusting the length of strip and the position of the triangular patch, a wideband end-fire CP antenna is successfully realized. Compared with other design methods, the proposed scheme, employing a loaded shorted triangular patch and stacked substrates, exhibits the advantages of compact antenna size, simple planar structure, easy processing, and low cost.

C. PARAMETRIC ANALYSIS OF THE PROPOSED END-FIRE CP ANTENNA

It is found that some key parameters have a significant impact on antenna performance, such as the distance between magnetic dipole plane to electric dipole plane $d = L_2/2 + L_3/2$, the length of offset parallel strip $L_{s1} + L_{s2}$, substrate length L_1, dielectric thickness $h = h_1 + h_2 + h_3$, and the shape of parallel strip, etc.

The magnitude and phase of the end-fire CP radiation can be tuned significantly using the parallel strip line, because it serves as a channel connecting magnetic dipole and electric dipole. Therefore, a parametric study on the parallel strip with and without offset is implemented as illustrated in Fig. 4 to further explore the working principle of the antenna. For the parallel strip, the phase difference between E_φ and E_θ varies from 60° to 140° within the operating frequency range, while the phase difference of the offset parallel strip maintains

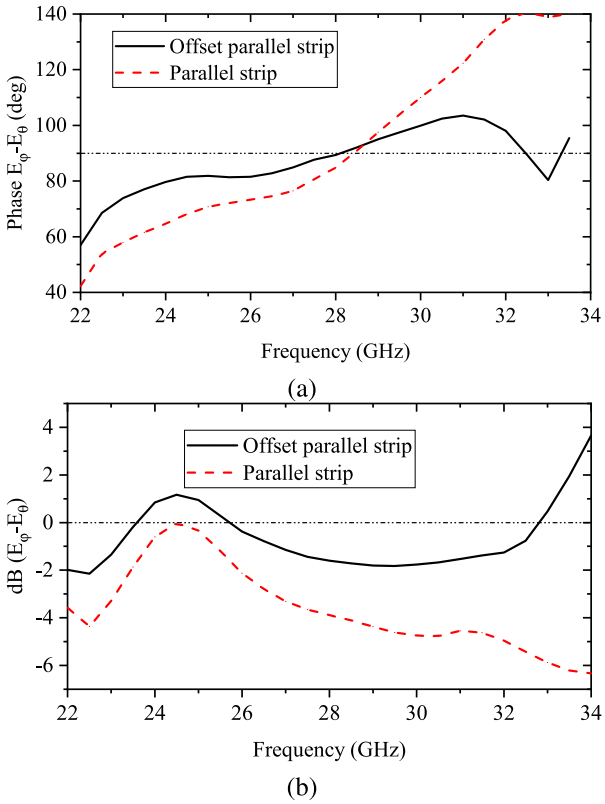

FIGURE 4. Effects of parallel strip with and without offset on the radiation fields of the proposed end-fire CP antenna, (a) amplitude difference and (b) phase difference between E_φ and E_θ.

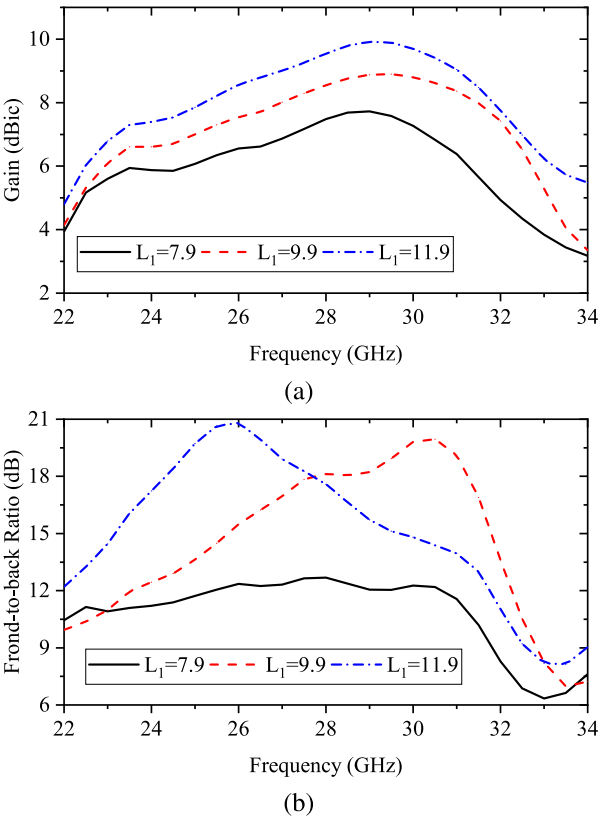

FIGURE 6. Simulated gain and FTBR of the proposed end-fire CP antenna with various L_1.

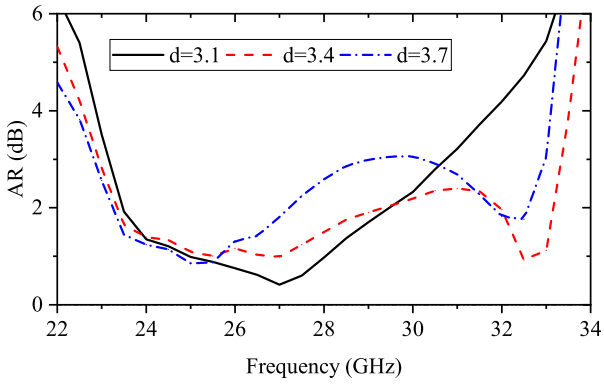

FIGURE 5. Simulated AR of the end-fire CP antenna with various d.

close to 90°, as shown in Fig. 4(a). Fig. 4(b) illustrates the amplitude ratio of these two electric fields. Notably, identical amplitudes is observed only in the low frequency when using parallel strip, whereas E_φ exhibits a smaller amplitude in other frequency band. As a contrast, the horizontal electric field component E_φ effectively excited through offset parallel strip in the high frequency band. Therefore, the wideband CP characteristic is formed by the novel offset parallel strip structure.

The distance d between the electric dipole and the magnetic dipole is another important factor for consideration. Fig. 5 shows the simulated AR performance with varied d values. The two orthogonal electric fields are work together when d is small. With the distance d increases, the CP resonant point, influenced by the electric dipole, gradually shifts to higher frequency band, forming the wideband AR performance. However, as the distance continues to increase, the AR performance in middle frequency band will deteriorate, leading to a failure to meet the CP conditions. The electric dipole cannot be effectively excited because of its location outside the coupling region of the offset parallel strip. This also demonstrated that the designed shorted triangular patch mainly influences the middle and high frequency bands.

In addition to wideband AR performance, gain is another crucial characteristic for end-fire CP antenna. Gain performance is related to its physical length, especially in the end-fire configuration [17]. FTBR parameter is employed to evaluate the backward radiation characteristic. A high FTBR value in the end-fire CP antenna system helps reduce interference between antennas and microwave circuits. Fig. 6 illustrates the simulated gain and FTBR characteristics of the end-fire CP antenna with the variation of substrate length L_1. As shown in Fig. 6(a), the CP gain is proportional to its length. Consequently, incorporating a dielectric rod can transform the proposed antenna into a wideband high-gain end-fire CP antenna. The substrate length also influences the FTBR property, as depicted in Fig. 6(b). For smaller values of L_1, the FTBR increases with the enhancement of antenna length L_1. However, as the substrate length further increases, the FTBR indicator remains essentially constant.

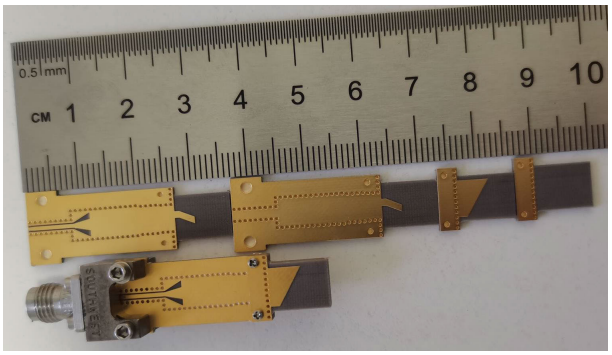

(a)

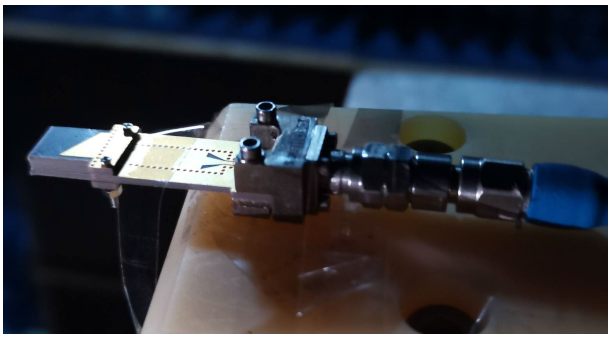

(b)

FIGURE 7. A photograph of the fabricated prototype and the measurement in far-field chamber.

Hence, careful consideration of antenna length should be given during the design of end-fire CP antenna.

III. EXPERIMENTAL RESULTS AND DISCUSSION

A. ANTENNA PROTOTYPE AND MEASUREMENT RESULTS

A photo of fabricated antenna prototype and the measurement in far-field chamber is exhibited in Fig. 7 to validate the performance of the proposed SIW end-fire CP antenna. A southwest end-launch connector is used for measurement by a transition structure of a ground coplanar waveguide (GCPW) to SIW. The reflection coefficient of the antenna under test (AUT) is measured by Agilent E8363B vector network analyzer (VNA) and the radiation patterns are measured in a microwave anechoic chamber. The antenna is designed by stacking three substrates of Taconic TLY with all ϵ_r = 2.2 and loss tangent = 0.0009. The low-cost single-layer PCB process is used to fabricate each substrate layer. Three fabricated substrate layers are stacked and assembled together with metal screws for measurement.

Measured and simulated reflection coefficients are illustrated in Fig. 8(a). As can be observed, the measured -10 dB reflection coefficient is from 23.8 GHz to 34 GHz, and the simulated one is from 23.9 GHz to 34 GHz. Measured and simulated results of AR and left-handed circular polarization (LHCP) gain are shown in Fig. 8(b) and (c). Good agreement between the measured and simulated ARs and gains are observed. The measured and simulated AR bandwidths are 38.6%, from 22.8 GHz to 33.7 GHz and 37.7% from

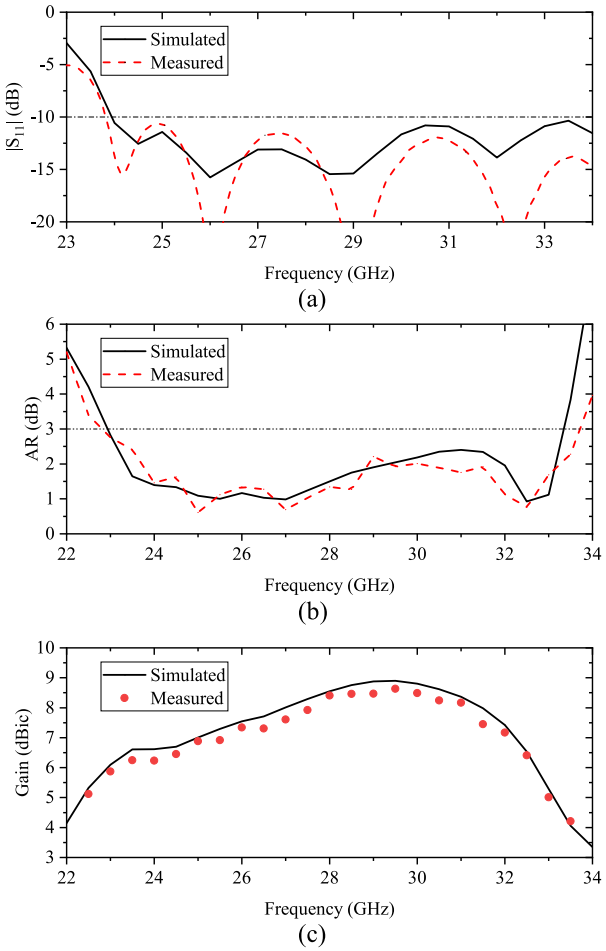

FIGURE 8. Measured and simulated performance of the proposed SIW end-fire CP antenna, (a) reflection coefficients, (b) AR, (c) LHCP gain.

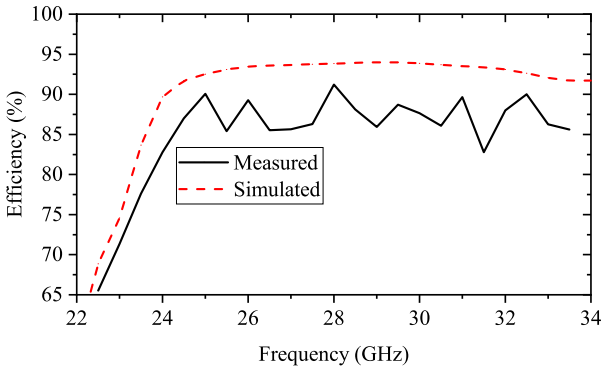

FIGURE 9. Measured and simulated radiation efficiencies of the proposed SIW end-fire CP antenna.

22.8 GHz to 33.4 GHz, respectively. The measured and simulated gain bandwidths are 35.7%, from 22.8 GHz to 32.7 GHz, and the 35%, from 22.9 GHz to 32.6 GHz, respectively. The measured and simulated peak LHCP gain is 8.6 dBic and 8.9 dBic appearing at 29.5 GHz, respectively.

Fig. 9 illustrates the measured and simulated radiation efficiencies of the proposed end-fire CP antenna. The measured radiation efficiency is achieved by comparing the measured LHCP gain and the simulated LHCP directivity.

TABLE 1. Comparison between proposed antenna and reported end-fire CP antennas.

Ref.	Antenna radiator	Geometry features	Ant. num.	Freq. (GHz)	Imp. BW %	AR. BW %	Max.G (dBic)	Aperture ($\lambda_0 \times \lambda_0$)	Length (λ_0)	Feb. cost
[13]	Offset parallel stripline	Single PCB	7	10	>3.1	3.1	10.3	0.18×0.05	6.6	low
[14]	Dielectric rod	3D printed dielectric	1	6	60.3	> 57	11.5	0.4×0.4	3.5	high
[15]	Stub-loaded dipole	Single PCB	1	2.45	24.8	18.8	3	0.8×0.033	0.88	low
[18]	Dipoles and metal block	PCB and metal	8	63.9	26	23.8	15.3	0.8×0.77	0.34	middle
[19]	Complementary yagi array	Single PCB	1	4.9	13.1	10.5	8	1.01×0.47	1.1	low
[20]	V-shaped dipole	Single PCB	1	2.6	5	25	6.1	1.48×0.034	1.17	low
[21]	Magneto-electric dipole	Single PCB	1	48	49.6	36.6	9.3	1.04×0.25	1.02	low
[22]	Horn and parasitic strips	Single PCB	1	27	16	>22	10.6	1.13×0.14	1.71	low
[23]	Tapered slot	Single PCB	1	95	31.5	34.7	9.6	3.5×0.25	3.16	low
[25]	Dipole and tapered slot	PCB and metal	8	33.5	42.1	35.8	14.1	0.69×0.62	0.56	middle
[28]	Log-periodic helix array	PCB and metal	1	1.9	50	46	6.1	0.53×0.11	2.24	high
[35]	Dielectric-loaded stepped slot	Stacked PCB	4	37.5	29.3	22.5	12.8	0.75×0.38	1.01	low
[37]	Magneto-electric dipole	Single PCB	4	60	28.5	24.6	10.4	0.88×0.2	0.48	low
Prop.	Slot and triangular patch	Stacked PCB	1	28	>35.3	38.6	8.6	0.75×0.28	0.92	low

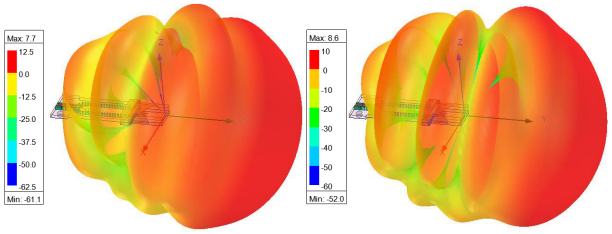

(a) (b)

FIGURE 10. Simulated 3D radiation patterns of the proposed SIW end-fire CP antenna, (a) 26 GHz, (b) 30 GHz.

It is observed that the peak measured radiation efficiency of the end-fire CP antenna is 91.2%, appearing at 28 GHz. The simulated 3D radiation patterns are depicted in Fig. 10, confirming that the proposed antenna has stable end-fire performance.

The measured and simulated normalized radiation patterns at different frequencies are plotted in Fig. 11. A good agreement is achieved between the measured and simulated results. There are some small bulges or depressions in the measured LHCP and RHCP radiation patterns, which mainly caused by imperfections environment and testing errors.

B. COMPARISON AND DISCUSSION

A comparison between the proposed antenna and other reported end-fire CP antennas in terms of antenna radiator, geometry features, size, fabricated cost, and electrical performance is summarized in Table 1. The aperture is defined as the product of its width along the x-axis direction and its thickness along the z-axis direction, while the antenna length corresponds to the length along the y-axis direction. The gain can be increased by extending the axial length along y-axis direction without changing the aperture size. For the fabricated cost, it should be selected these antennas with planar structure and simple regular geometry, such as [13], [15], [20], and [22]. Reference [21] focuses on good performance, such as wideband S_{11} and AR performance. Other references implement almost excellent operating bandwidth by introducing non-planar structure [28]

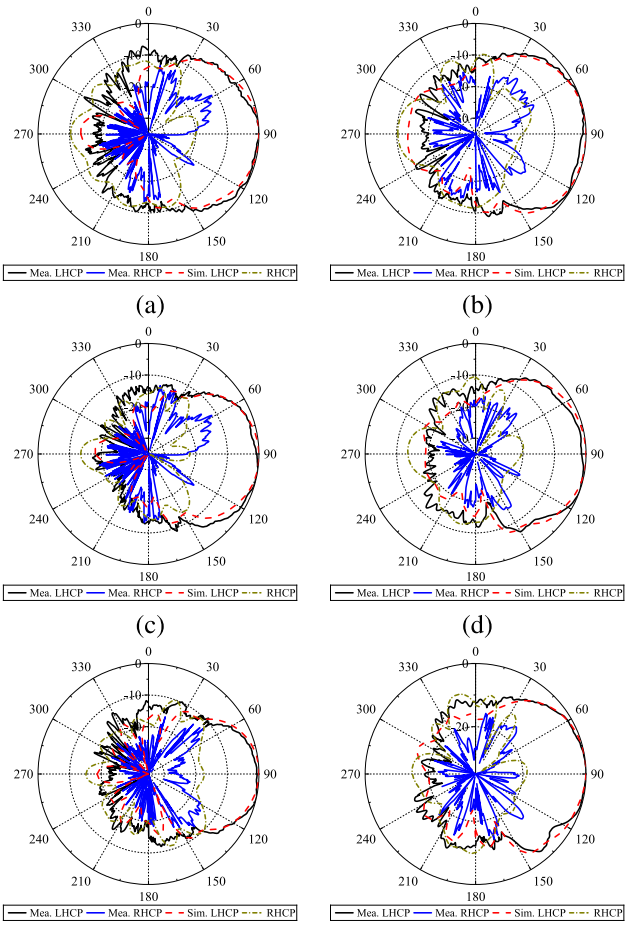

FIGURE 11. Measured and simulated radiation patterns of the proposed array, (a) xy plane at 25 GHz, (b) yz plane at 25 GHz, (c) xy plane at 28 GHz, (d) yz plane at 28 GHz, (e) xy plane at 31 GHz, (f) yz plane at 31 GHz.

or new manufacturing process [14] for new resonant end-fire CP structure and new machining process verification. Some researches have carried out valuable exploration for novel planar end-fire CP radiation pattern [19], dual-CP and multibeam capacity [35], [37]. Considering manufacturing processes, some references [18] and [25] suggest the combination of planar and non-planar antenna structures,

whereas others [23] only utilize mechanically processed microwave device structure to design end-fire CP antennas.

Compared with the latest end-fire CP antenna reported in recent years, the proposed antenna may have some interesting highlights, such as novel shorted triangular patch, novel design of offset parallel strip, stacked substrates for antenna miniaturization, excellent performance, frequency selection flexibility, and easy integration characteristics, which makes it an attractive candidate on end-fire CP antenna design for mm-wave wireless systems.

IV. CONCLUSION

In this paper, a novel planar wideband CP antenna loaded shorted triangular patch has been proposed and investigated for mm-wave end-fire radiation. By employing an open-ended SIW, a pair of stacked substrates and shorted triangular patches, and an offset parallel strip, the proposed antenna has successfully implemented end-fire CP radiation pattern with a wide AR bandwidth. To understand the CP working principle, an electric dipole and a magnetic dipole have been used for explanation. Additionally, the key parameters have been discussed in the design. A prototype has been fabricated and measured, achieving wide impedance bandwidth and AR bandwidth, novel shorted triangular patch and offset parallel strip design structure, compact antenna size, stable radiation patterns, frequency selection flexibility, as well as easy fabrication and integration. Compared with latest end-fire CP antennas, it can be concluded that the proposed end-fire CP antenna is an attractive candidate for future wideband mm-wave applications.

REFERENCES

[1] S. Chen, S. Sun, and S. Kang, "System integration of terrestrial mobile communication and satellite communication—The trends, challenges and key technologies in B5G and 6G," *China Commun.*, vol. 17, no. 12, pp. 156–171, Dec. 2020.

[2] W. Hong, Z. H. Jiang, C. Yu, D. Hou, H. Wang, C. Guo, Y. Hu, L. Kuai, Y. Yu, Z. Jiang, Z. Chen, J. Chen, Z. Yu, J. Zhai, N. Zhang, L. Tian, F. Wu, G. Yang, Z.-C. Hao, and J. Y. Zhou, "The role of millimeter-wave technologies in 5G/6G wireless communications," *IEEE J. Microw.*, vol. 1, no. 1, pp. 101–122, Jan. 2021.

[3] U. Ullah, M. Al-Hasan, S. Koziel, and I. B. Mabrouk, "Series-slot-fed circularly polarized multiple-input–multiple-output antenna array enabling circular polarization diversity for 5G 28 GHz indoor applications," *IEEE Trans. Antennas Propag.*, vol. 69, no. 9, pp. 5607–5616, Sep. 2021.

[4] L. Wei, R. Q. Hu, Y. Qian, and G. Wu, "Key elements to enable millimeter wave communications for 5G wireless systems," *IEEE Wireless Commun.*, vol. 21, no. 6, pp. 136–143, Dec. 2014.

[5] J. Zeng, Z. Zhang, F. H. Lin, and F. Guan, "Penta-mode ultrawideband circularly polarized stacked patch antennas using characteristic mode analysis," *IEEE Trans. Antennas Propag.*, vol. 70, no. 10, pp. 9051–9060, Oct. 2022.

[6] Y. Xu, L. Zhu, N.-W. Liu, and L.-L. Qiu, "An inductively coupled CP slot antenna based on intrinsic 90° phase difference and its flexible application in wideband CP radiation," *IEEE Trans. Antennas Propag.*, vol. 71, no. 2, pp. 1204–1215, Feb. 2023.

[7] E. Baghernia, M. M. M. Ali, and A. R. Sebak, "2 × 2 slot spiral cavity-backed antenna array fed by printed gap waveguide," *IEEE Access*, vol. 8, pp. 170609–170617, 2020.

[8] C. Q. Zhang and L. Y. Feng, "Design of high gain magneto-electric dipole antenna by loading a magneto-electric dipole director," *IEEE Antennas Wireless Propag. Lett.*, vol. 22, no. 8, pp. 1823–1827, Aug. 2023.

[9] W.-W. Yang, W.-J. Sun, H. Tang, and J.-X. Chen, "Design of a circularly polarized dielectric resonator antenna with wide bandwidth and low axial ratio values," *IEEE Trans. Antennas Propag.*, vol. 67, no. 3, pp. 1963–1968, Mar. 2019.

[10] H. Xu, J. Zhou, K. Zhou, Q. Wu, Z. Yu, and W. Hong, "Planar wideband circularly polarized cavity-backed stacked patch antenna array for millimeter-wave applications," *IEEE Trans. Antennas Propag.*, vol. 66, no. 10, pp. 5170–5179, Oct. 2018.

[11] W.-J. Lu, J.-W. Shi, K.-F. Tong, and H.-B. Zhu, "Planar endfire circularly polarized antenna using combined magnetic dipoles," *IEEE Antennas Wireless Propag. Lett.*, vol. 14, pp. 1263–1266, 2015.

[12] M. You, W.-J. Lu, B. Xue, L. Zhu, and H.-B. Zhu, "A novel planar endfire circularly polarized antenna with wide axial-ratio beamwidth and wide impedance bandwidth," *IEEE Trans. Antennas Propag.*, vol. 64, no. 10, pp. 4554–4559, Oct. 2016.

[13] S. Ge, Q. Zhang, A. K. Rashid, Y. Zhang, M. Yu, and R. Murch, "Low-profile high-gain endfire antenna with circular polarization," *IEEE Trans. Antennas Propag.*, vol. 70, no. 8, pp. 7181–7186, Aug. 2022.

[14] J. Huang, S. J. Chen, Z. Xue, W. Withayachumnankul, and C. Fumeaux, "Wideband circularly polarized 3-D printed dielectric rod antenna," *IEEE Trans. Antennas Propag.*, vol. 68, no. 2, pp. 745–753, Feb. 2020.

[15] J. Zhang, W. Lu, L. Li, L. Zhu, and H. Zhu, "Wideband dual-mode planar endfire antenna with circular polarisation," *Electron. Lett.*, vol. 52, no. 12, pp. 1000–1001, Jun. 2016.

[16] W.-H. Zhang, W.-J. Lu, and K.-W. Tam, "A planar end-fire circularly polarized complementary antenna with beam in parallel with its plane," *IEEE Trans. Antennas Propag.*, vol. 64, no. 3, pp. 1146–1152, Mar. 2016.

[17] J. Wang, Y. Li, L. Ge, J. Wang, M. Chen, Z. Zhang, and Z. Li, "Millimeter-wave wideband circularly polarized planar complementary source antenna with endfire radiation," *IEEE Trans. Antennas Propag.*, vol. 66, no. 7, pp. 3317–3326, Jul. 2018.

[18] X. Ruan and C. H. Chan, "An endfire circularly polarized complementary antenna array for 5G applications," *IEEE Trans. Antennas Propag.*, vol. 68, no. 1, pp. 266–274, Jan. 2020.

[19] W. Zhou, J. Liu, and Y. Long, "A broadband and high-gain planar complementary Yagi array antenna with circular polarization," *IEEE Trans. Antennas Propag.*, vol. 65, no. 3, pp. 1446–1451, Mar. 2017.

[20] W.-J. Lu, K. Wang, S.-S. Gu, L. Zhu, and H.-B. Zhu, "Directivity enhancement of planar endfire circularly polarized antenna using V-shaped 1.5-wavelength dipoles," *IEEE Antennas Wireless Propag. Lett.*, vol. 18, no. 7, pp. 1420–1423, Jul. 2019.

[21] Y. Tian, J. Ouyang, P. F. Hu, and Y. Pan, "Millimeter-wave wideband circularly polarized endfire planar magneto-electric dipole antenna based on substrate integrated waveguide," *IEEE Antennas Wireless Propag. Lett.*, vol. 21, no. 1, pp. 49–53, Jan. 2022.

[22] S. Xu, G. Jin, J. Yang, and S. Liao, "Wideband high-gain low-profile endfire linearly/circularly polarized antennas based on magnetic dipole directors for millimeter-wave applications," *IEEE Antennas Wireless Propag. Lett.*, vol. 22, no. 4, pp. 854–858, Apr. 2023.

[23] X. Cheng, Y. Yao, J. Yu, and X. Chen, "Circularly polarized substrate-integrated waveguide tapered slot antenna for millimeter-wave applications," *IEEE Antennas Wireless Propag. Lett.*, vol. 16, pp. 2358–2361, 2017.

[24] Y. Yao, X. Cheng, J. Yu, and X. Chen, "Analysis and design of a novel circularly polarized antipodal linearly tapered slot antenna," *IEEE Trans. Antennas Propag.*, vol. 64, no. 10, pp. 4178–4187, Oct. 2016.

[25] Y. Yu, Z. H. Jiang, J.-D. Zhang, and W. Wu, "Broadband millimeter-wave endfire circularly polarized array with a low-profile feeding structure," *IEEE Trans. Antennas Propag.*, vol. 70, no. 8, pp. 7270–7275, Aug. 2022.

[26] Y. Yin and K. Wu, "Endfire circularly-polarized antipodal linearly tapered slot antenna fed by slotted width-tapered SIW," *IEEE Trans. Antennas Propag.*, vol. 70, no. 4, pp. 2411–2421, Apr. 2022.

[27] S. S. Hesari and J. Bornemann, "Wideband circularly polarized substrate integrated waveguide endfire antenna system with high gain," *IEEE Antennas Wireless Propag. Lett.*, vol. 16, pp. 2262–2265, 2017.

[28] Z. Chen, Z. Hu, L.-H. Ye, and D.-L. Wu, "Wideband circularly polarized endfire antenna based on counter-wound normal-mode helix," *IEEE Trans. Antennas Propag.*, vol. 70, no. 3, pp. 1797–1805, Mar. 2022.

[29] L. Wang, Y.-C. Jiao, and Z. Weng, "Novel dual-band circularly polarized planar endfire antenna with enhanced front-to-back ratios," *IEEE Trans. Antennas Propag.*, vol. 70, no. 2, pp. 969–976, Feb. 2022.

[30] J.-Y. Zhang, J.-D. Zhang, Q.-Y. Chen, W. Wu, and D.-G. Fang, "Broadband millimeter-wave circularly polarized open-ended waveguide antenna using stubs and its application in forming an array," *IEEE Trans. Antennas Propag.*, vol. 71, no. 1, pp. 542–549, Jan. 2023.
[31] W.-H. Zhang, P. Cheong, W.-J. Lu, and K.-W. Tam, "Planar endfire circularly polarized antenna for low profile handheld RFID reader," *IEEE J. Radio Freq. Identificat.*, vol. 2, no. 1, pp. 15–22, Mar. 2018.
[32] X. Cheng, Y. Yao, T. Tomura, J. Hirokawa, T. Yu, J. Yu, and X. Chen, "A compact multi-beam end-fire circularly polarized septum antenna array for millimeter-wave applications," *IEEE Access*, vol. 6, pp. 62784–62792, 2018.
[33] Y. Yang, Y.-L. Ban, X. Li, Q. Sun, and C.-Y.-D. Sim, "Millimeter-wave endfire wide-angle scanning circularly polarized antenna array," *IEEE Antennas Wireless Propag. Lett.*, vol. 21, no. 11, pp. 2219–2223, Nov. 2022.
[34] J. Hu, Z.-C. Hao, K. Fan, and Z. Guo, "A bidirectional same sense circularly polarized endfire antenna array with polarization reconfigurability," *IEEE Trans. Antennas Propag.*, vol. 67, no. 11, pp. 7150–7155, Nov. 2019.
[35] Q. Wu, J. Hirokawa, J. Yin, C. Yu, H. Wang, and W. Hong, "Millimeter-wave multibeam endfire dual-circularly polarized antenna array for 5G wireless applications," *IEEE Trans. Antennas Propag.*, vol. 66, no. 9, pp. 4930–4935, Sep. 2018.
[36] A. Wang, L. Yang, Y. Zhang, X. Li, X. Yi, and G. Wei, "A novel planar dual circularly polarized endfire antenna," *IEEE Access*, vol. 7, pp. 64297–64302, 2019.
[37] F. Y. Xia, Y. J. Cheng, Y. F. Wu, and Y. Fan, "V-band wideband circularly polarized endfire multibeam antenna with wide beam coverage," *IEEE Antennas Wireless Propag. Lett.*, vol. 18, no. 8, pp. 1616–1620, Aug. 2019.
[38] M. Ye, X.-R. Li, and Q.-X. Chu, "Single-layer single-fed endfire antenna with bidirectional circularly polarized radiation of the same sense," *IEEE Antennas Wireless Propag. Lett.*, vol. 16, pp. 621–624, 2017.
[39] R. K. Jaiswal, A. K. Ojha, K. Kumari, K. V. Srivastava, and C.-Y.-D. Sim, "Wideband bidirectional same sense endfire circularly polarized antenna," *IEEE Access*, vol. 10, pp. 65801–65808, 2022.

HENGFEI XU (Member, IEEE) received the B.S. degree in electronic information science and technology from Yantai University, in 2008, the M.S. degree in electromagnetic field and microwave technology from the University of Electronic Science and Technology of China (UESTC), Chengdu, China, in 2011, and the Ph.D. degree in electromagnetic field and microwave technology from Southeast University, Nanjing, China, in 2018. From 2011 to 2012, he was a Research Engineer of power amplifiers and microwave passive components with Huawei Technology Company Ltd. He is currently a Lecturer with the Department of Information and Communication Engineering, Nanjing Institute of Technology. His current research interests include the microwave and millimeter-wave circuits and antennas.

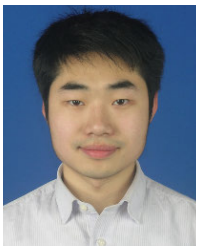

BOYU SIMA (Member, IEEE) received the B.S. and M.S. degrees from the Nanjing University of Science and Technology, Nanjing, China, in 2010 and 2013, respectively, and the Ph.D. degree from Nanjing University, Nanjing, in 2019. Since 2019, he has been with the Nanjing University of Science and Technology (NJUST) as a Research Assistant. His current research interests include metamaterials, metasurface, liquid crystal-based antennas, and retroreflector arrays.

PU WEI received the B.S. degree in automation and the Ph.D. degree in electrical engineering from Southeast University, Nanjing, China, in 2004 and 2011, respectively. Currently, he is an Associate Professor with the Department of Communication Engineering, Nanjing Institute of Technology. His current research interests include wireless communication and optical communication.

LEI TANG was born in Jiangsu, China, in 1981. She received the Ph.D. degree from the Nanjing University of Aeronautics and Astronautics (NUAA), in 2014. Currently, she is an Associate Professor with the School of Communication Engineering, Nanjing Institute of Technology, China. Her current research interests include channel coding and signal processing for wireless communications.

SHU JIANG received the B.S. and Ph.D. degrees in electromagnetic field and microwave technology from the State Key Laboratory of Millimeter Waves, Southeast University, Nanjing, China, in 2010 and 2017, respectively.

From 2018 to 2019, she was a Transceiver Engineer with ZTE Corporation. Since 2019, she has been with the School of Information and Communication Engineering, Nanjing Institute of Technology. Her current research interests include microwave and millimeter-wave circuits, antennas, and front-end subsystems.

CHUANQING LIU received the B.S. degree in physics from the University of Hubei, Wuhan, China, in 1987, and the M.S. and Ph.D. degrees in information and communication engineering from the Huazhong University of Science and Technology, Wuhan, in 1999 and 2006, respectively. Since 2007, he has been a Professor with the School of Information and Communication Engineering and a Master Advisor with the Nanjing Institute of Engineering. His current research interests include RF technology, systems in mobile communications, and the Internet of Things.